

THREE-WAVE INTERACTIONS OF DISTURBANCES IN A HYPERSONIC BOUNDARY LAYER ON A POROUS SURFACE

S. A. Gaponov and N. M. Terekhova

UDC 532.526

Interactions of disturbances in a hypersonic boundary layer on a porous surface are considered within the framework of the weakly nonlinear stability theory. Acoustic and vortex waves in resonant three-wave systems are found to interact in the weak redistribution mode, which leads to weak decay of the acoustic component and weak amplification of the vortex component. Three-dimensional vortex waves are demonstrated to interact more intensively than two-dimensional waves. The feature responsible for attenuation of nonlinearity is the presence of a porous coating on the surface, which absorbs acoustic disturbances and amplifies vortex disturbances at high Mach numbers. Vanishing of the pumping wave, which corresponds to a plane acoustic wave on a solid surface, is found to assist in increasing the length of the regions of linear growth of disturbances and the laminar flow regime. In this case, the low-frequency spectrum of vortex modes can be filled owing to nonlinear processes that occur in vortex triplets.

Key words: *hypersonic boundary layer, three-wave resonance systems, acoustic and vortex disturbances.*

Introduction. It is known that the use of various wavy and porous surfaces, slotted suction, and heated and cooled surfaces substantially affects the character of disturbance development in boundary layers. Possible consequences are, on the one hand, suppression of various disturbances and longer regions of the laminar flow and, on the other hand, intensification of exchange processes and turbulization of the boundary layer (see [1, 2]). Therefore, it seems reasonable to examine these factors for the purpose of solving problems of boundary-layer control in practice.

Experiments [3] performed in a T-326 hypersonic wind tunnel of the Khristianovich Institute of Theoretical and Applied Mechanics of the Siberian Division of the Russian Academy of Sciences should be noted, where the composition and dynamics of disturbances along the boundary layer on solid impermeable and porous surfaces at hypersonic Mach numbers were studied. The porous coating was found to affect the disturbance dynamics at the linear and nonlinear stages of disturbance evolution. At high Mach numbers, there appear spatially growing disturbances induced by excitation of acoustic oscillations in addition to natural oscillations (traveling Tollmien–Schlichting vortex waves, which are the first-mode disturbances). The most intensely growing mode of these acoustic oscillations in the examined flow regimes is the second mode (see [4]).

Bountin et al. [3] demonstrated that the linear stage of disturbance development in the boundary layer on a solid impermeable surface is followed by the stage of nonlinear interaction in three-wave systems. There are several triplets in this case. The first triplet relates the plane wave of the second mode with the frequency parameter F_{II} to the pair of oblique waves of the first mode at the subharmonic half-frequency (frequency parameter $F_{II/2}$). The second triplet relates the acoustic wave with the frequency parameter F_{II} to two vortex waves: the most intensely growing component with the frequency parameter F_I and the vortex component with the parameter $F_{II} - F_I$ (the

Khristianovich Institute of Theoretical and Applied Mechanics, Siberian Division, Russian Academy of Sciences, Novosibirsk 630090; gaponov@itam.nsc.ru; terekh@itam.nsc.ru. Translated from *Prikladnaya Mekhanika i Tekhnicheskaya Fizika*, Vol. 50, No. 5, pp. 3–13, September–October, 2009. Original article submitted May 27, 2008; revision submitted October 24, 2008.

subscripts I and II refer to the first and second mode, respectively). Nonlinear processes lead to a fairly rapid emergence of the transitional regime with a subsequent transition to turbulence.

Another pattern was observed in experiments on a porous surface. The porous coating was found to extend the linear stage of disturbance development. The nonlinearity is rather weak, and there are no dominating frequencies determining the process intensity and direction. A theoretical analysis can reveal the reasons for different types of disturbance evolution. Gaponov et al. [5] performed such an analysis for a solid impermeable surface within the framework of the linear stability theory. In a hypersonic boundary layer on such a surface, nonlinear interaction is found to occur between the acoustic and vortex waves in the parametric resonance regime. The pumping wave is a plane acoustic wave of the second mode, whose growth in the linear region is much more intense than that of the vortex wave. When the pumping wave intensity reaches a certain threshold value, nonlinear interactions of this wave with subharmonic vortex components begin, which may lead to packet growth of the Tollmien–Schlichting waves. This interaction is more intense if the vortex waves are three-dimensional.

The activities described in the present paper involved numerical simulations of the linear and nonlinear stages of disturbance evolution on a porous surface. Weakly nonlinear interactions of two types were considered: between the acoustic and vortex modes (see [5]) and between the vortex modes with filling of the subharmonic low-frequency spectrum, which is detected in experiments [3] by bispectral methods. The experimental parameters [3] were used as the initial conditions: boundary layer on a cone with a cone half-angle approximately equal to 7° , free-stream velocity corresponding to $M = 5.95$, unit Reynolds number $Re_1 = 12.5 \cdot 10^6 \text{ m}^{-1}$, and streamwise Reynolds numbers corresponding to the experimental values.

Constitutive Relations and Methods of the Solution. The basic postulates of the nonlinear model of interaction of disturbances in three-wave resonance systems in boundary layers of a compressible gas were described in detail in [6]. Only some indispensable information is given below. Let us denote the scale of the fluctuating field by ε ($\varepsilon \ll 1$). Disturbed fields of velocity \bar{u} , density $\bar{\rho}$, pressure \bar{p} , and temperature \bar{T} of a compressible gas,

$$\begin{aligned} \bar{u} &= |U(Y) + \varepsilon u', \varepsilon v', \varepsilon w'|, & \bar{\rho} &= \rho(Y) + \varepsilon \zeta', & \bar{p} &= P(Y) + \varepsilon p', \\ \bar{T} &= T(Y) + \varepsilon \Theta', & p'/P &= \zeta'/\rho + \Theta'/T \end{aligned}$$

are considered in a dimensionless Cartesian coordinate system (X, Y, Z) : $X = x/\delta$, $Y = y/\delta$, and $Z = z/\delta$ ($\delta = \sqrt{\nu_e x/U_e}$ is the characteristic scale; the subscript e refers to parameters on the boundary-layer edge; the primed and non-primed quantities are the fluctuating and mean values, respectively). The solution is found by means of expansion with respect to the small parameter ε and two-scale expansion of the streamwise coordinate. In addition to the “fast” scale X , we introduced a “slow” scale $\xi = \varepsilon X$ because of significant differences in the rate of changes in the disturbance phase and amplitude.

The solutions for the waves are sought in the form

$$\bar{Z}'_j = A_j(\xi) \bar{Z}_j^0(Y) \exp(i\theta_j) + \text{c. c.} + \varepsilon(\bar{Z}'_j)^1 + \dots, \quad j = 1, 2, 3, \quad (1)$$

where $\bar{Z} = |u, v, w, p, \Theta|$ are the amplitude eigenfunctions of the streamwise, normal, and transverse components of the wave velocities and pressure and temperature disturbances; A is a slowly changing amplitude; the complex conjugate quantities are denoted by c. c.; $\theta = \alpha X + \beta Z - \omega t$; $\alpha = \alpha^r + i\alpha^i$; $\alpha^i < 0$ is the growth rate; the frequency $\omega = 2\pi f$ is a real quantity; the wavenumbers α and β are related to the frequency by the dispersion relation $\alpha = \alpha(\omega, \beta)$ of the linear theory.

From the full system of equations of motion and conservation laws for a compressible gas [4], we obtain the following initial recurrent system for the vector function \bar{Z} within the framework of the weakly nonlinear theory [6]:

$$\begin{aligned} \varepsilon \left[\sum_{j=1}^n \exp(i\theta_j) \left(L(\bar{Z}_j^0) + \frac{\partial L(\bar{Z}_j^0)}{\partial \alpha_j} \frac{\partial}{\partial X} + \frac{\partial L(\bar{Z}_j^0)}{\partial \omega_j} \frac{\partial}{\partial t} \right) A_j \right. \\ \left. + \varepsilon \sum_{k,l}^n \exp(i(\theta_k + \theta_l)) [L(\bar{Z}_{k+l}^1) + A_k A_l \bar{Q}_{k,l}^j(\bar{Z}_j^0 \bar{Z}_{lX}^0, \dots)] \right] = 0. \end{aligned} \quad (2)$$

The expressions for the linear operator L have the form

$$[\rho(Gu + U_Y v) + i\alpha p/(\gamma M^2) - (\mu/\text{Re})u_{YY}] \exp(i\theta) = 0,$$

$$\begin{aligned}
[\rho G w + i\beta p/(\gamma M^2) - (\mu/\text{Re})w_{YY}] \exp(i\theta) &= 0, & [\rho G v + p_Y/(\gamma M^2)] \exp(i\theta) &= 0, \\
[G\zeta + \rho_Y v + \rho(i\alpha u + v_Y + i\beta w)] \exp(i\theta) &= 0, & & (3) \\
[\rho(G\Theta + T_Y v) + (\gamma - 1)(i\alpha u + v_Y + i\beta w) - \mu\gamma/(\sigma \text{Re})\Theta_{YY}] \exp(i\theta) &= 0, \\
\zeta = \rho(p/P - \Theta/T), & & G = i(-\omega + \alpha U).
\end{aligned}$$

In Eqs. (2) and (3), M is the Mach number on the boundary-layer edge, $\gamma = c_P/c_V$ is the ratio of specific heats, $\sigma = c_P\mu_e/k$ is the Prandtl number, k is the thermal conductivity, and \bar{Q} is the sum of the nonlinear terms of the initial equations.

The boundary conditions for disturbances have the form $\{u, w, \Theta\} = 0$ and $v = v(p)$ at $Y = 0$ or $\{u, v, w, \Theta\} = 0$ at $Y = \infty$. At hypersonic Mach numbers $M > 5$, the boundary-layer thickness is determined by the value $Y \approx 17$, and integration is performed in the interval $0 \leq Y \leq Y_k$ ($Y_k = 25$). All quantities are normalized to parameters on the boundary-layer edge; the following normalization was chosen for eigenfunctions: $|v|_{Y_k} = 1$.

In the case of the first-order disturbances with respect to ε , using the eighth-order homogeneous system (3) (the so-called Dann–Lin system), we can find the eigenvalues of α for specified values of β , ω , and Reynolds numbers $\text{Re} = x/\delta$ ($\text{Re} = \sqrt{R_X}$) and also determine the amplitude eigenfunctions of the linear waves (1) with a non-specified amplitude parameter A .

Applying the standard Squire transform [4] $\alpha u + \beta w = \bar{\alpha}\bar{u}$, $\alpha v = \bar{\alpha}\bar{v}$, $\alpha p = \bar{\alpha}\bar{p}$, $\alpha\zeta = \bar{\alpha}\bar{\zeta}$, $\alpha^2 + \beta^2 = \bar{\alpha}^2$, $\alpha \text{Re} = \bar{\alpha}R$, $\alpha M = \bar{\alpha}\bar{M}$, and $\alpha\bar{\omega} = \bar{\alpha}\bar{\omega}$, we reduce system (3) to an equivalent problem for two-dimensional disturbances, namely, to the sixth-order Lees–Lin system:

$$\begin{aligned}
\rho(G\bar{u} + U_Y\bar{v}) + i\bar{\alpha}\bar{p}/(\gamma\bar{M}^2) - (\mu/R)\bar{u}_{YY} &= 0, & \rho G\bar{v} + \bar{p}_Y/(\gamma\bar{M}^2) &= 0, \\
G\bar{\zeta} + \rho_Y\bar{v} + \rho(i\bar{\alpha}\bar{u} + \bar{v}_Y) &= 0, \\
\rho(G\Theta + T_Y\bar{v}) + (\gamma - 1)(i\bar{\alpha}\bar{u} + \bar{v}_Y) - \mu\gamma/(\sigma R)\Theta_{YY} &= 0, \\
\bar{\zeta} = \rho(\bar{p}/P - \Theta/T), & & G = i(-\bar{\omega} + \bar{\alpha}U).
\end{aligned}$$

Let us specify the boundary conditions for this system: conditions of disturbance decay at infinity $\{\bar{u}, \bar{v}, \Theta\} = 0$ at high values of the streamwise coordinate ($Y \gg 0$), the no-slip condition along the surface $\{\bar{u}, \Theta\} = 0$ (the plate is permeable only in the normal direction) and the condition derived from the equation of motion and permeability law $\bar{v}(0) = K\bar{p}(0)$ [7–9] on the wall ($Y = 0$).

Several models were proposed for determining the coefficient K . Two of them were described in [7]. In the present work, we use the model [8, 9] applied for simulations of compressible gases. We consider a perforated plate with pore diameters \bar{r}_1 and small (as compared with the boundary-layer thickness) distances between the pores. The pores are shaped as cylinders and are oriented normal to the plate surface. The pore length is sufficiently small to assume that the pressure distribution in the pores is independent of the radial direction.

In determining the value of K for compressible gases, we used the laws of propagation of acoustic waves in long narrow channels, which are characterized by the propagation constant λ and the characteristic impedance Z_0 . Daniels [10] obtained the values of λ and Z_0 expressed via the acoustic parameters: impedance of the tube element Z and coefficient W characterizing the reserve of the compression energy and the loss due to heat transfer to the walls. These acoustic parameters characterize the ratio between the bulk velocity averaged over the tube (pore) cross section and the pressure. According to [8], the expressions for Z and W can be presented in the dimensionless form as

$$Z = i\bar{\alpha}c \frac{I_0(\sqrt{i\bar{\alpha}cR}r_1)}{I_2(\sqrt{i\bar{\alpha}cR}r_1)}, \quad W = -i\bar{\alpha}cM^2 \left(\gamma + (\gamma - 1) \frac{I_2(\sqrt{i\bar{\alpha}cR\sigma}r_1)}{I_0(\sqrt{i\bar{\alpha}cR\sigma}r_1)} \right),$$

where I_0 and I_2 are the zeroth- and second-order Bessel functions, and r_1 is the ratio of the pore radius to the boundary-layer thickness. Then, $\lambda = \sqrt{ZW}$ and $Z_0 = Z/\lambda$. Let the relation $\bar{p}(-H) = X_1 v_1(-H)$ be specified on one end of the pore. Then, we have

$$\frac{v_1(0)}{\bar{p}(0)} = \frac{Z_0 - X_1 \tanh(\lambda H)}{Z_0(Z_0 \tanh(\lambda H) - X_1)}.$$

If the fraction of the surface occupied by pores (porosity) is n , then the flow velocity near the surface is $\bar{v}(0) = nv_1(0)$; hence, we obtain

$$K = \frac{\bar{v}(0)}{\bar{p}(0)} = \frac{n(Z_0 - X_1 \tanh(\lambda H))}{Z_0(Z_0 \tanh(\lambda H) - X_1)}.$$

It makes sense to determine the value of X_1 if we consider the porosity on the surface adjacent to a large volume with no averaged motion of the gas (e.g., to a chamber with low-intensity suction). In the case of a porous surface on an impermeable wall (see [3]), we have $X_1 = \infty$; therefore, $K = n \tanh(\lambda H)/Z_0$.

Solving this boundary-value problem, finding α at given Re , ω , and β , and constructing the amplitude eigenfunctions of the waves in accordance with [3], we can consider that the laws of disturbance evolution in the linear region are known. The weakly nonlinear theory predicts that nonlinearity in the situation with the above-indicated sought parameters affects only the wave amplitude A .

The resonance model is based on the process of paired interaction of waves in the field of the third wave under the condition of synchronization of their phases: $\theta_j = \theta_k + \theta_l$. In the case of disturbances of the second order with respect to ε , we can find higher-order disturbances \bar{Z}^1 from the inhomogeneous equations (2) and also (using the solubility conditions) construct the amplitude equations for resonance triads similar to the system derived in [6]. For a simple three-wave system of j -, k -, and l -waves (usually $j \neq k \neq l$), these equations have the form

$$\begin{aligned} \frac{dA_j}{d\xi} &= -\alpha_j^i A_j + S_{k,l}^j A_k A_l \exp(i\Delta), \\ \frac{dA_k}{d\xi} &= -\alpha_k^i A_k + S_{j,l}^k A_j A_l^* \exp(i\Delta), \quad \frac{dA_l}{d\xi} = -\alpha_l^i A_l + S_{j,k}^l A_j A_k^* \exp(i\Delta), \end{aligned} \quad (4)$$

$$S_{k,l}^j = \int_0^{Y_k} \bar{Z}_j^{0+} \bar{Q}_{k,l}^j dY \quad / \quad \int_0^{Y_k} \bar{Z}_j^{0+} \frac{\partial L(\bar{Z}_j^0)}{\partial \alpha_j} dY, \quad \Delta = \int (\alpha_k + \alpha_l - \alpha_j)^r dX,$$

where Δ is the phase synchronization factor, which takes into account the possibility of detuning in terms of wavenumbers in triplets, and \bar{Z}^{0+} are the solutions of the adjoint system of equations with respect to system (3).

In this work, the dimensionless frequency parameter F related to frequency by the dependence $\omega = \text{Re } F$ and the reduced dimensional wavenumber $b = 10^3 \beta / \text{Re}$ are constant for each wave mode. Both plane (two-dimensional) waves with $b = 0$ and oblique (three-dimensional) waves with $b \neq 0$, which have the maximum growth rate at this frequency, are considered.

In Eqs. (4), the initial values of the amplitudes A_j of the traveling waves were defined via the initial intensities I of the wave components. The relation between the oscillation amplitudes and intensity is expressed in terms of the calculated value of the mass velocity fluctuations m : $I_j(\xi_0) = A_j(\xi_0) m_j(Y_m) \exp(-\alpha_j^i \xi_0)$.

The mass velocity fluctuations $m = \rho u + \zeta U$ were assumed to reach the maximum level for the prevailing wave component (this component is found from the amplitude-frequency spectrum of disturbances). The value of the mean mass velocity $\rho U(Y_m)$ is calculated numerically, and the initial intensities I_j are assumed to be expressed in fractions of ρU . The initial wave amplitudes are varied in a wide range.

Results and Discussion. The experiments [3] were performed in the boundary layer on a cone with the free-stream Mach number $M = 5.95$. This value decreases behind the oblique shock wave and reaches $5.30 \leq M \leq 5.35$ on the boundary-layer edge. The measurements were performed in the range $3.5 \cdot 10^7 \leq R_X \leq 5.3 \cdot 10^7$. The stagnation temperature in the experiments was constant and equal to 390 K, $\gamma = 1.4$, and the Prandtl number was $\sigma = 0.72$. Our calculations were performed with the same parameters.

Two variants of the problem were considered: evolution of disturbances on a flat plate and on a cone. At different values of the streamwise coordinate, the boundary-layer thicknesses on a flat plate and on a cone are known to be identical, and $x^{\text{pl}} = x^{\text{con}}/3$. Therefore, we used $\partial/\partial\xi = (1/2) \partial/\partial \text{Re}$ for the plate and $\partial/\partial\xi = (1/6) \partial/\partial \text{Re}$ for the cone in Eqs. (4). The presence of these coefficients in the right sides of Eqs. (4) affects the character of nonlinear growth of amplitudes in the cases considered. System (4) was solved in the interval $1080 \leq \text{Re} \leq 1400$, which is slightly wider than the range of measurements [3].

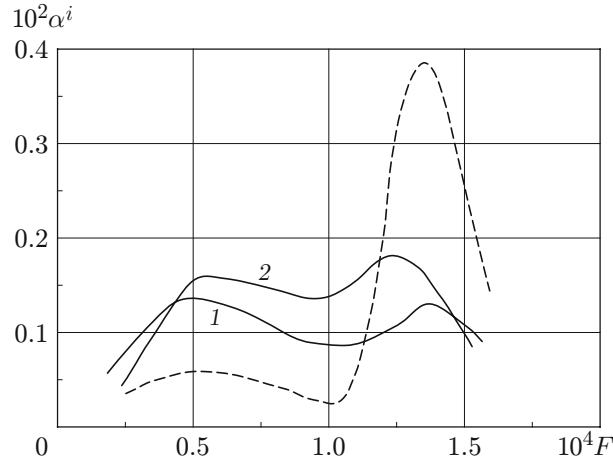


Fig. 1. Growth rates α^i of two-dimensional linear waves ($b = 0$) for different frequencies ($\text{Re} = 1080$ and $M = 5.35$): the solid curves shows the results for a porous surface with $n = 0.5$ (1) and 0.75 (2); the dashed curve shows the data for a solid impermeable surface [5].

Let us consider the linear eigenvalues of disturbances of the first and second modes on a porous surface. Figure 1 shows the growth rates α^i of two-dimensional waves ($b = 0$) calculated by Eqs. (3) with $M = 5.35$ and $\text{Re} = 1080$ as functions of the frequency parameter F (solid curves) and also the linear growth rates of disturbances on a solid impermeable surface [5] (dashed curve). The dimensionless pore radius corresponds to the pore radius in [3]. The range of the frequency parameter $1.1 \leq 10^4 F \leq 1.6$ corresponds to the second-mode acoustic disturbances, and the range of the frequency parameter $10^4 F \approx 0.5\text{--}0.7$ corresponds to the first-mode vortex disturbances. It follows from Fig. 1 that the second-mode growth rates on an impermeable surface are much higher than the growth rates of the Tollmien–Schlichting waves. The evolution of disturbances at these Mach and Reynolds numbers, therefore, is completely determined by acoustic waves.

In the case of a porous surface, the growth rates of the second-mode acoustic waves decrease, while the growth rates of the first-mode vortex waves are more than doubled. For this reason, the vortex disturbances display the most intense growth. Such dependences are typical for supersonic regimes with moderate Mach numbers. Curve 1 in Fig. 1 agrees with the results obtained by Fedorov et al. [7]; these data were used in the major part of the calculations.

For the first-mode vortex waves, as for an impermeable surface [5], the location of the maximum $\alpha_{\max}^i(F)$ remains unchanged with increasing Re and corresponds to the value $F_1 \approx 0.59 \cdot 10^{-4}$. In the case of the second-mode acoustic waves on a porous wall (in contrast to an impermeable wall), the frequency parameter F is not constant: it increases in the downstream direction. The maximum value of α^i changes insignificantly in the downstream direction (within 5–10%); it decreases for vortex components and increases for acoustic components.

Some characteristics are identical for both impermeable and porous surfaces, in particular, the phase velocities of disturbances ($c_{\text{I}} \approx 0.88$ and $c_{\text{II}} \approx 0.92$) and the location of the maximum of the mass velocity fluctuations m [the maximum of the second mode is located closer to the boundary-layer edge ($Y \approx 16$) than the maximum of the first mode ($Y \approx 12$)]. The effect of the wave type on the streamwise amplification factor is retained. Figure 2 shows the growth rates α^i of two-dimensional and three-dimensional waves of the first and second modes on the wave parameter b for $M = 5.35$, $\text{Re} = 1080$, and $n = 0.5$. It is seen that the growth rates of three-dimensional components for the first mode exceed the growth rates of two-dimensional components, and the growth rate α^i reaches the maximum value at $b = 0.14$. This value corresponds to the angle of inclination of the wave vector to the main flow approximately equal to 45° , which agrees with the measurement data on the most dangerous angles. Among the second-mode waves, the most unstable ones are plane two-dimensional waves with $b = 0$. These results are valid for all frequencies and Reynolds numbers.

The results of comparisons performed in [7] show that the calculated amplification factor for the second mode in the boundary layer on a cone are in good agreement with experimental data. The differences are observed

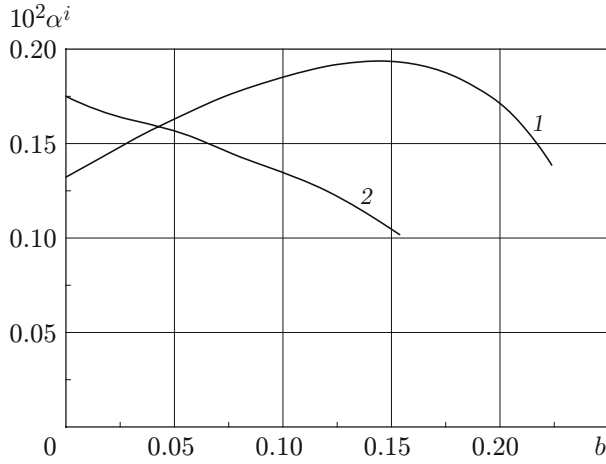


Fig. 2

Fig. 2. Linear growth rates α^i of the traveling Tollmien–Schlichting waves with $F = 0.59 \cdot 10^{-4}$ (1) and the second-mode waves with $F = 10^{-4}$ (2) versus the wave parameter b for $\text{Re} = 1080$, $M = 5.35$, and $n = 0.5$.

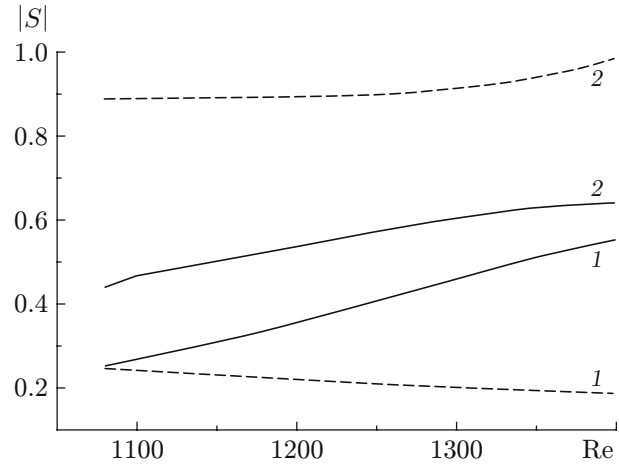


Fig. 3

Fig. 3. Absolute value of the nonlinear relation coefficient versus the Reynolds number ($M = 5.35$ and $n = 0.5$) for the second-mode disturbances with $F_{II} = 1.2 \cdot 10^{-4}$ (solid curves) and for the vortex disturbances with $F_{II/2} = 0.6 \cdot 10^{-4}$ (dashed curves) in different triplets formed by two-dimensional acoustic waves interacting with vortex waves: curves 1 and 2 refer to the two-dimensional wave ($b = 0$) and three-dimensional wave ($b = \pm 0.14$), respectively.

at high Reynolds numbers at the end of the observation interval, where the experimental values are substantially lower than the calculated data.

Figure 3 shows the dependence $|S|(\text{Re})$ for the first triplet considered, which relates the second-mode two-dimensional wave (we will call it the harmonic with the frequency parameter $F_{II} = 1.2 \cdot 10^{-4}$) to the first-mode vortex waves (subharmonics with $F_{II/2} = 0.6 \cdot 10^{-4}$), with the above-indicated values of the Mach number, Reynolds number, and porosity. Both two-dimensional vortex waves with $b = 0$ (curves 1) and three-dimensional vortex waves with $b = \pm 0.14$ (curves 2) are considered in this triplet at the subharmonic frequency. The coefficients $|S_{2,3}^1|$ for the acoustic harmonic with F_{II} refer to the solid curves in Fig. 3, and the coefficients $|S_{1,3}^2| = |S_{1,2}^3|$ for vortex subharmonics refer to the dashed curves in Fig. 3.

It is clear that nonlinear interaction in such triplets is more intense if three-dimensional waves are formed at the subharmonic frequency, because the nonlinear relation coefficients are higher than the corresponding coefficients for two-dimensional waves by an order of magnitude.

The growth rates and the nonlinear relation coefficients for triplets of the second type, which relate the second-mode harmonic with F_{II} to the first-mode wave (component with the maximum growth rate F_I and component with the difference frequency F_{II-I}) are found to be insignificantly different from the corresponding characteristics of the above-considered subharmonic triplet. It may be expected, therefore, that the dynamics of these vortex components along the boundary layer will be identical in the case of identical initial intensity.

Nonlinear interactions described by system (4) are also considered. The calculations are performed for the following values of the frequency parameter: $F_{II} = 1.35 \cdot 10^{-4}$, $1.20 \cdot 10^{-4}$, and $1.10 \cdot 10^{-4}$. As $F_I = 0.59 \cdot 10^{-4}$, we can easily determine the frequency parameters $F_{II/2}$ and F_{II-I} in these triplets.

Nonlinear interaction of waves of the first and second mode on a porous surface is found to be substantially different from interaction of the same waves on a solid impermeable surface: it is extremely weak. For the nonlinear process to start, the wave intensity should be more than 1% of the mean mass velocity ρU (in the case of hypersonic velocities, these values are rather high). Below these threshold values, the wave evolution follows the linear laws, and the nonlinearity observed alters the wave amplitude by less than 1%.

It should also be noted that the energy is always transferred to the subharmonic region, independent of the initial values of the amplitudes and the relations between them at various frequencies. There is practically no

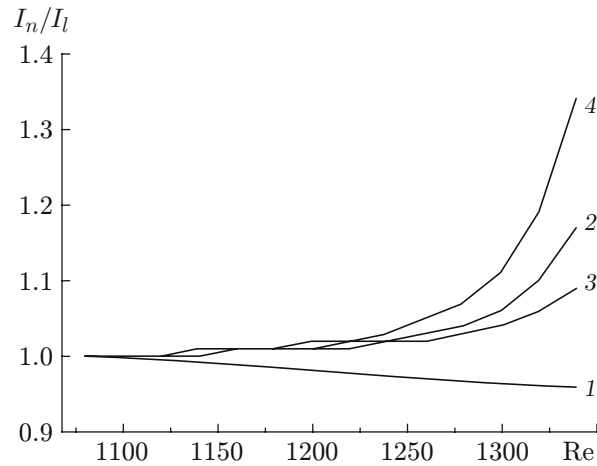


Fig. 4. Ratio of nonlinear and linear intensities of interacting waves I_n/I_l versus the Reynolds number Re for the first triplet (curves 1 and 2) and second triplet (curves 1, 3, and 4) for $M = 5.35$ and $n = 0.5$: two-dimensional acoustic wave with $F_{II} = 1.1 \cdot 10^{-4}$ (1), three-dimensional vortex wave with $F_{II/2} = 0.55 \cdot 10^{-4}$ and $b = \pm 0.14$ (2), three-dimensional vortex wave with $F_I = 0.59 \cdot 10^{-4}$ and $b = 0.14$ (3), and three-dimensional vortex wave with $F_{II-I} = 0.51 \cdot 10^{-4}$ and $b = -0.14$ (4).

nonlinearity in the boundary layer on a flat plate even at high initial wave intensities (approximately 1% of the mean mass velocity ρU). Therefore, only the data obtained in the boundary layer on a cone are given further.

Naturally, nonlinearity is primarily manifested if there are three-dimensional vortex waves at the subharmonic frequency; the increase in amplitude for plane waves is smaller by an order of magnitude (see Fig. 3).

Figure 4 shows the ratio of nonlinear intensity (I_n) and linear intensity (I_l) as a function of the Reynolds number for two triplets composed from the harmonic, which is the second-mode acoustic wave with $F_{II} = 1.1 \cdot 10^{-4}$ (curve 1), and three-dimensional vortex waves with $F_{II/2} = 0.55 \cdot 10^{-4}$ (curve 2) and $F_I = 0.59 \cdot 10^{-4}$ (curve 3) and $F_{II-I} = 0.51 \cdot 10^{-4}$ (curve 4). Nonlinear interaction is rather weak in the major part of the range of Reynolds numbers considered and is amplified only at the end of the interval, where the calculated values of the growth rates α^i are unreliable, as was mentioned above.

In this case, the difference mode of the second triplet is amplified to the greatest extent, but it is not always so: different local amplifications of one or another vortex component are observed at different frequencies, which may lead to the emergence of local peaks with moderate values. As a result of this energy redistribution, the intensity of the acoustic component becomes slightly lower than the linear intensity. For comparison, it should be noted that the nonlinear growth of the vortex components in such triplets on a solid impermeable surface acquires an explosive character already at $Re \approx 1200$ even for substantially smaller initial intensities [5].

Figure 5 shows similar dependences for triplets with the acoustic-mode frequency parameter $F_{II} = 1.2 \cdot 10^{-4}$ for the vortex-component parameters $F_{II/2} = 0.6 \cdot 10^{-4}$, $F_I = 0.59 \cdot 10^{-4}$, and $F_{II-I} = 0.61 \cdot 10^{-4}$. It follows from Fig. 5 that the intensities of the subharmonic components again change only weakly in the major part of the considered range of Reynolds numbers considered and increase at the end of this interval for the reasons discussed above. As the subharmonic frequencies are rather close to each other, the intensities of the vortex components almost coincide.

In those cases where triplets of different types are formed, their comparative estimates should be performed. For this purpose, we need to introduce the notion of the effective amplitude or effective intensity and compare the quantity $I_{\text{eff}} = \sqrt{(I_{F_I}^2 + I_{F_{II-I}}^2)}/2$ or $I_{\text{eff}} = (I_{F_I} + I_{F_{II-I}})/2$ with the disturbance intensity at the half-frequency $F_{II/2}$. The estimates show that the value of I_{eff} under the conditions considered exceeds the value of $I_{F_{II/2}}$ by several percent. This allows us to confirm the preliminary conclusion (made in considering the nonlinear relation coefficients) that the effectiveness of the considered triplets is almost identical.

Figure 6 shows the interaction of the first-mode three-dimensional vortex wave with F_I , which is a harmonic in this triplet, with its two-dimensional and three-dimensional subharmonics with $F_{I/2}$, whose amplitudes are smaller than the harmonic amplitude by an order of magnitude. In such a triplet, only the two-dimensional vortex

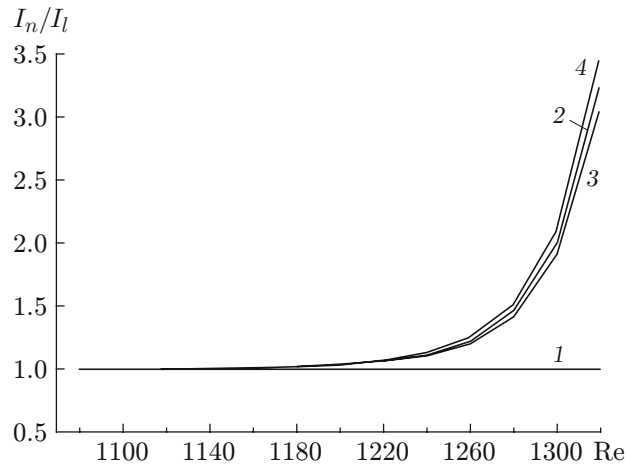


Fig. 5. Ratio of nonlinear and linear intensities of interacting waves I_n/I_l versus the Reynolds number Re for the first triplet (curves 1 and 2) and second triplet (curves 1, 3, and 4) for $M = 5.35$ and $n = 0.5$: two-dimensional acoustic wave with $F_{II} = 1.2 \cdot 10^{-4}$ (1), three-dimensional vortex wave with $F_{II/2} = 0.6 \cdot 10^{-4}$ and $b = \pm 0.14$ (2), three-dimensional vortex wave with $F_I = 0.59 \cdot 10^{-4}$ and $b = 0.14$ (3), and three-dimensional vortex wave with $F_{I-I} = 0.61 \cdot 10^{-4}$ and $b = -0.14$ (4).

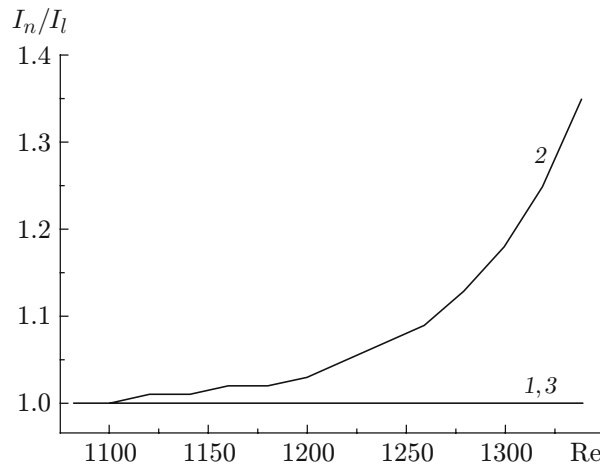


Fig. 6. Ratio of nonlinear and linear intensities of interacting vortex waves I_n/I_l on the Reynolds number Re for $M = 5.35$ and $n = 0.5$: three-dimensional vortex wave with $F_I = 0.59 \cdot 10^{-4}$ and $b = 0.14$ (curve 1) and subharmonic vortex waves with $F_{I/2} = 0.295 \cdot 10^{-4}$ (curves 2 and 3) (curve 2 refers to the two-dimensional component with $b = 0$ and curve 3 refers to the three-dimensional component with $b = 0.14$).

subharmonic component can be expected to exhibit nonlinear growth (curve 2). The harmonic and the three-dimensional vortex subharmonic component increase in accordance with the linear law (curves 1 and 3).

In addition, the interaction of waves in triplets with two-dimensional and three-dimensional vortex components in different combinations is considered. Nonlinear interaction is found to be possible for different vortex waves, but it is rather weak (as in the case considered) and is manifested at the end of the examined range of Reynolds numbers.

Based on the discussion above, we can state that the conclusions drawn from the experiments [3] are confirmed theoretically. In the flow around a cone with a porous surface, the nonlinear interaction of acoustic and

vortex waves in a hypersonic boundary layer is extremely weak and occurs in the regime of energy redistribution between the acoustic and vortex components, which leads to insignificant decay of the acoustic component and moderate enhancement of the vortex components. Such interaction is more intense in the case of three-dimensional vortex waves. The decrease in nonlinearity is caused by the presence of a porous coating, which absorbs acoustic disturbances at hypersonic Mach numbers, attenuates acoustic disturbances of the second mode, and amplifies vortex disturbances (obviously, owing to changes in the Reynolds stresses and their gradient along the normal in the near-wall region).

Vanishing of the pumping wave (which corresponds to a plane acoustic wave on a solid surface) results in a longer laminar flow regime and in more extended regions of the linear growth of disturbances. In this case, three-wave system can display nonlinear interaction of the vortex components and also filling of the low-frequency spectrum of the vortex modes.

This work was supported by the Russian Foundation for Basic Research (Grant No. 08-01-00038a).

REFERENCES

1. A. V. Boiko, G. R. Grek, A. V. Dovgal', and V. V. Kozlov, *Origination of Turbulence in Near-Wall Flows* [in Russian], Nauka, Novosibirsk (1999).
2. Y. S. Kachanov, "Physical mechanisms of laminar-boundary-layer transition," *Ann. Rev. Fluid Mech.*, **26**, 411–482 (1994).
3. D. A. Bountin, A. N. Shipliyuk, A. A. Maslov, and N. Chokani, "Nonlinear aspects of hypersonic boundary layer stability on a porous surface," AIAA Paper No. 0258 (2004).
4. S. A. Gaponov and A. A. Maslov, *Development of Disturbances in Compressible Flows* [in Russian], Nauka, Novosibirsk (1980).
5. S. A. Gaponov, N. M. Terekhova, and B. V. Smorodskii, "Three-wave interaction of disturbances in a hypersonic boundary layer," *Vestn. Novosib. Gos. Univ., Ser. Fiz.*, **3**, No. 3, 39–45 (2008).
6. S. A. Gaponov and I. I. Maslennikova, "Subharmonic instability of a supersonic boundary layer," *Teplofiz. Aéromekh.*, **4**, No. 1, 1–10 (1997).
7. A. Fedorov, A. Shipliyuk, A. Maslov, et al., "Stabilization of a hypersonic boundary layer using an ultrasonically absorptive coating," *J. Fluid Mech.*, **479**, 99–124 (2003).
8. S. A. Gaponov, "Effect of gas compressibility on the stability of a boundary layer above a permeable surface at subsonic velocities," *J. Appl. Mech. Tech. Phys.*, **16**, No. 1, 95–98 (1975).
9. S. A. Gaponov, "Effect of properties of a porous coating on boundary-layer stability," *Izv. Sib. Otd. Akad. Nauk SSSR, Ser. Tekh. Nauk*, No. 3, Issue 1, 21–23 (1971).
10. F. B. Daniels, "On the propagation of sound waves in a cylindrical conduit," *J. Acoust. Soc. Amer.*, **44**, 563–564 (1950).